# cmgh

## ORIGINAL RESEARCH

# Cysteine Protease-Mediated Autocleavage of *Clostridium difficile* Toxins Regulates Their Proinflammatory Activity

Yongrong Zhang,[1] Shan Li,[1] Zhiyong Yang,[1] Lianfa Shi,[1] Hua Yu,[1]
Rosangela Salerno-Goncalves,[2] Ashley Saint Fleur,[1] and Hanping Feng[1]

[1]Department of Microbial Pathogenesis, School of Dentistry, [2]Department of Pediatrics and Center for Vaccine Development, School of Medicine, University of Maryland, Baltimore, Maryland
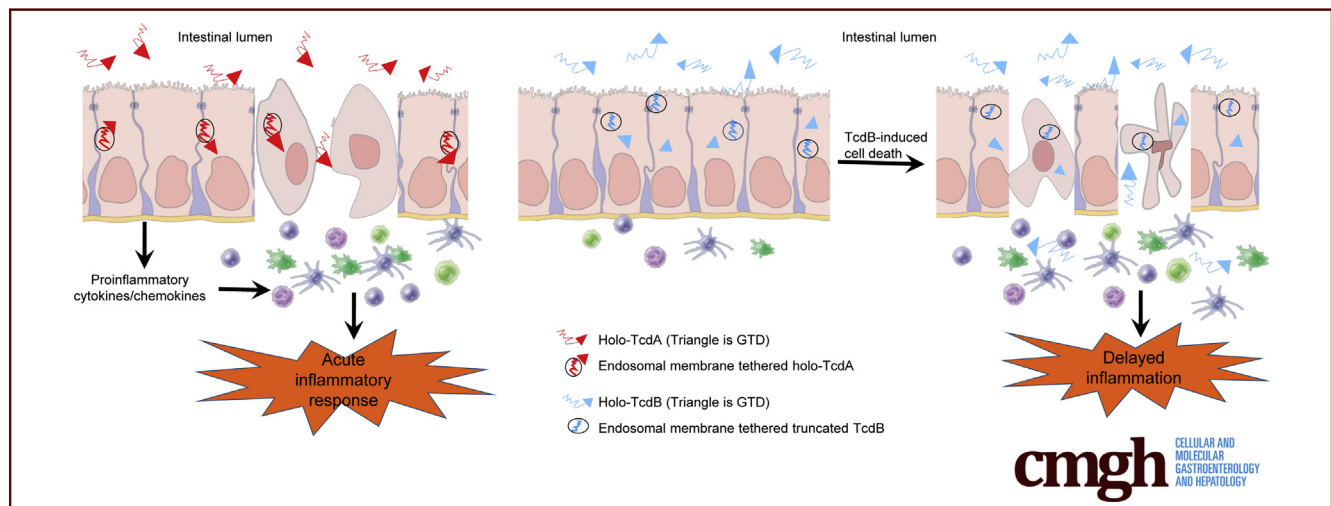


## SUMMARY

This study identified an unexpected function of *Clostridium difficile* toxin autoprocessing that regulates in vivo inflammatory activities of *C difficile* toxin A and toxin B. The differential autoprocessing mediated by the cysteine proteases of the 2 toxins plays a role on the regulation of their major bioactivities.

**BACKGROUND & AIMS:** *Clostridium difficile* toxin A (TcdA) and *C difficile* toxin toxin B (TcdB), the major virulence factors of the bacterium, cause intestinal tissue damage and inflammation. Although the 2 toxins are homologous and share a similar domain structure, TcdA is generally more inflammatory whereas TcdB is more cytotoxic. The functional domain of the toxins that govern the proinflammatory activities of the 2 toxins is unknown.

**METHODS:** Here, we investigated toxin domain functions that regulate the proinflammatory activity of *C difficile* toxins. By using a mouse ilea loop model, human tissues, and immune cells, we examined the inflammatory responses to a series of chimeric toxins or toxin mutants deficient in specific domain functions.

**RESULTS:** Blocking autoprocessing of TcdB by mutagenesis or chemical inhibition, while reducing cytotoxicity of the toxin, significantly enhanced its proinflammatory activities in the animal model. Furthermore, a noncleavable mutant TcdB was significantly more potent than the wild-type toxin in the induction of proinflammatory cytokines in human colonic tissues and immune cells.

**CONCLUSIONS:** In this study, we identified a novel mechanism of regulating the biological activities of *C difficile* toxins in that cysteine protease-mediated autoprocessing regulates toxins' proinflammatory activities. Our findings provide new insight into the pathogenesis of *C difficile* infection and the design of therapeutics against the disease. *(Cell Mol Gastroenterol Hepatol 2018;5:611–625; https://doi.org/10.1016/j.jcmgh.2018.01.022)*

*Keywords: C difficile; Toxins; Cysteine Protease; Autoprocessing; Inflammation.*

*C*lostridium difficile, an anaerobic gram-positive, spore-forming bacterium that can induce fatal intestinal inflammatory disease, is the most prevalent cause of antibiotic-associated diarrhea and pseudomembranous colitis in nosocomial settings.[1] Two exotoxins, toxin A (TcdA) and toxin B (TcdB), secreted by the bacterium, are primarily responsible for the induction of disease because strains lacking both toxins are avirulent.[2] TcdA and TcdB are large homologous single-chain proteins that contain at least 4 distinct domains[3]: an N-terminal glucosyltransferase

domain (GTD), a cysteine protease domain (CPD), a putative translocation domain, and a C-terminal receptor binding domain (RBD). Although the exact method of toxin entry into target cells remains elusive, a model of toxin action is emerging[3]: after receptor-mediated endocytosis, which may involve regions in both the translocation domain and RBD,[4,5] the CPD and GTD eventually are translocated into the cytosol where cysteine protease self-cleaves and releases GTD from the rest of the toxin. GTD inactivates Rho guanosine triphosphatases, leading to the intoxication of host cells. Thus, CPD plays a key role in the cytosolic delivery of GTD effectors. Autoprocessing-deficient TcdA or TcdB mutants are still cytotoxic to host cells inducing cell rounding, Rho guanosine triphosphatase glucosylation, and apoptosis, but such activity is reduced compared with their wild-type toxins.[6,7]

*C difficile* infection (CDI) is typified by diarrhea, intestinal inflammation, and tissue damage, and in severe cases pseudomembranous colitis. Toxin-induced intestinal inflammation, a hallmark of CDI, is characterized by the production of proinflammatory cytokines/chemokines, neutrophil infiltration, and intestinal epithelial damage.[8] Both TcdA and TcdB are proinflammatory; however, TcdB induces markedly weaker inflammatory responses than TcdA. TcdA elicited neutrophil influx, extensive tissue damage, and fluid accumulation within a short incubation period in various animal gut loop models.[9–12] These acute enterotoxic responses, key characteristics of pseudomembranous colitis, thus defined TcdA as a major virulence factor in these earlier studies, although recent studies found that isogenic strains that express only TcdB induced more severe diseases in animals than those that express only TcdA.[13–15] In contrast, TcdB did not show such acute enterotoxicity in animal gut loop models[9–12,16,17] even though TcdB was a more potent cytotoxin than TcdA.[2,18] In a more recent study using a cecum injection model, TcdA but not TcdB could induce rapid cecal inflammation.[19] The precise mechanism controlling such differential inflammatory activities of the 2 toxins is unknown. In this study, we identified a previously unknown function of CPD as an internal regulator of the proinflammatory activity of *C difficile* toxins. By using a series of chimeric and enzyme-deficient holotoxins in a well-established mouse ileal loop model that clearly differentiates between responses to TcdA and to TcdB, we determined that CPD-mediated autoprocessing regulates the acute inflammatory responses to the 2 toxins. Moreover, we validated this result in human intestinal tissues and immune cells. Our finding thus provides new understanding of the molecular mechanism regulating *C difficile* toxin biological functions and insight into the pathogenesis of CDI.

# Materials and Methods
## Generation of Chimeric, Mutant, and Wild-Type Toxins

To study the domain functions of the 2 toxins, we generated several chimeric toxins and mutant toxins deficient of enzymatic activity. The gene encoding the RBD of TcdB was amplified by polymerase chain reaction (PCR) and inserted into plasmid pHis-TcdA to replace the RBD of TcdA using XmaI/SpeI sites, generating the plasmid encoding chimera TxA-Br, which is TcdA with the RBD replaced by TcdB's RBD. The primers used for generating TxA-Br were as follows: forward: 5'-AATTACTAGTA TAACCGGTTTTGTGACTGTAGGCGATG-3' and reverse: 5'-ATATCCCGGGTTAGTGATGGTGATGGTGATGCGATCC-3'.

To generate the chimera TxA-Bgt, which is TcdA with the GTD replaced by TcdB's GTD, a unique BamHI site was introduced into the position between GTD and CPD without changing the sequence of amino acids in pHis-TcdB by overlap PCR. The PCR product of TcdA without GTD was substituted into plasmid pHis-TcdB using BamHI/AgeI sites. The primer sets used for this construction were as follows: TcdB-forward1: 5'-TTTGTTTATCCACCGAACTAAG-3' sense, TcdB-reverse1: 5'-ACCAAGGGATCCTTCAAAATAATTCC-3'; TcdB-forward2: 5'-TTATTTTGAAGGATCCCTTGGTGAAG-3', TcdB-reverse2: 5'-GCTGCACCTAAAC TTACAC-3'; TcdA-forward: 5'-TGGTGGATCCCTTTCTGAAGAC-3', and TcdA-reverse: 5'-TGATTGGCTCCAATTCTTG-3'.

The CPD from TcdA was amplified, and TxB-ACPD (TcdB with the CPD replaced by TcdA's CPD) was generated by replacing the CPD of TcdB with this specific PCR product using restriction sites BamHI and Bpu10I, which are located at the beginning and end of TcdB's CPD. The primer sets used for this construction were TcdA544 BamHI-forward: 5'-GGATCCC TTTCTGAAGACAATGGGGTAGAC-3', and Bpu10I-TxA-CPD-reverse: 5'-AATTTGCTCAGGAATATTCTTGGACTTTGC-3'.

TcdB-C698S was generated as previously described.[20] The TcdB-L543A plasmid was a kind gift from Dr Aimee Shen (Tufts University). GTD deficient TcdA (aTcdA) was generated as previously described.[21]

The constructs carrying full-length wild-type, mutant, and chimeric toxin genes were used to transform *Bacillus megaterium*, and all holotoxins were expressed and purified using the same methods described previously.[21]

## Cell Lines and Cytotoxicity Assay

The African green monkey kidney Vero cell line was obtained from American Type Culture Collection. Cells were maintained in Dulbecco's modified Eagle medium containing 10% fetal bovine serum, 100 U/mL penicillin, 100 $\mu$g/mL streptomycin, 2 mmol/L L-glutamine, and 1 mmol/L sodium pyruvate. The cytotoxicity of toxins on cultured cells was assessed by cell rounding assays. Vero cells, seeded in 96-well plates, were treated with either holotoxins or chimeras. Cell rounding was visualized by phase-contrast

microscopy. Each holotoxin or chimera concentration was tested in triplicate for overall cell rounding, and the experiments were repeated 3 times.

## Mice and Ileal Loop Experiment

CD1 female mice (age, 6–8 wk) were purchased from Envigo (Frederick, MD) and housed in dedicated pathogen-free facilities. The mice were handled and cared for according to Institutional Animal Care and Use Committee guidelines.

Mice were fasted overnight before being deeply anesthetized with 100 mg/kg (body weight) ketamine and 10 mg/kg (body weight) xylazine. After a midline laparotomy, one 1- to 2-cm ileal loop was ligated and injected with 10 $\mu$g of wild-type, chimeric, or mutant toxins in 100 $\mu$L of phosphate-buffered saline (PBS). Control loops were injected with 100 $\mu$L of PBS alone. In some groups, AWP19[22] was added to the toxin solution at a final concentration of 5 $\mu$mol/L before injection into mouse ilea. Carboxytetramethylrhodamine (TAMRA)-labeled and nonfluorescent AWP19 were gifts from Dr Aimee Shen (Tufts University) and Dr Matthew Bogyo (Stanford School of Medicine). After 4 hours, the mice were euthanized and the ileal loops were removed for subsequent analysis. To measure fluid accumulation, the loop lengths and weights were measured, and fluid secretion was assessed based on the ratio of loop weight (mg) to loop length (cm). More than 5 mice were included in each experimental group. The experiments were repeated at least 3 times.

## Myeloperoxidase Assay

To measure neutrophil myeloperoxidase (MPO) activity, a portion of the resected ileum was freeze-dried and homogenized in 1 mL of 50 mmol/L PBS containing 0.5% hexadecyl trimethyl ammonium bromide and 5 mmol/L EDTA. The tissues from each mouse were disrupted with both sonication and freeze-thaw cycles. MPO activity in the centrifuged supernatant was determined using tetramethylbenzidine (TMB) peroxidase substrate (KPL, Gaithersburg, MD) followed by measuring the absorbance of the samples at 450 nm using a plate reader. MPO activity units were calculated according to the standard curve generated using purified MPO from human leukocytes (Sigma, St. Louis, MO).

## Reverse Transcription PCR Analysis of Cytokine Production

Total RNA from the intestine was extracted by an RNeasy Plus Mini kit (Qiagen, Hilden, Germany). The RNA was treated further with RQ1 RNase-free DNase (Promega, Madison, WI) to remove DNA contamination. The purified total RNA (1 $\mu$g) was reverse-transcribed to obtain complementary DNA using moloney murine leukemia virus (M-MLV) reverse transcriptase (Invitrogen, Carlsbad, CA) with oligo (deoxythymidine) for 1 hour at 37°C. PCR amplification was performed with the following conditions for 30 cycles: 94°C for 30 seconds, 55°C for 30 seconds, and 72°C for 30 seconds. All PCR reactions were performed with GoTaq Green Master Mix (Promega, Madison, MI). The following mouse-specific primer sets were used: interleukin (IL)-1$\beta$ primer sets (sense, 5'-CCCCAACTGGTACATCA-3'; antisense, 5'-AGGTAAGTGG TTGCCC-3'); IL-6 primer sets (sense, 5'-ATGATGGATGCTAC-CAAAC-3'; antisense, 5'-AGGCATAACGCACTAGG-3'); keratinocyte chemoattractant (KC, also known as mouse chemokine ligand 1 [CXCL1]) primer sets (sense, 5'-GAGCCTCTAACCAGTTCC-3'; antisense, 5'-GGCTATGACTT CGGTTTG-3'); and glyceraldehyde-3-phosphate dehydrogenase primer sets (sense, 5'-CCAAGGAGTAAGAAACCC-3'; antisense, 5'-GGTGCAGCGAACTTTATT-3').

## Histopathologic Analysis

Histopathologic analysis was performed to evaluate mucosal damage induced by the toxins. Resected ileal loops were fixed in 4% formaldehyde buffered with PBS, dehydrated through graded ethanol solutions, and embedded in paraffin. The tissues were sectioned and stained with H&E by the Electron Microscopy/Histology Laboratory (Department of Pathology, University of Maryland Baltimore). Overall damage was analyzed by a histologist who was blinded to the identity of each sample. A score of 0 to 4 was given to reflect the level of inflammation and epithelial damage: +1 indicated some inflammatory cells and/or some cellular debris in the lumen, extent of either in the lumen was less than 25% of the space; +2 indicated greater than 25% of the space in the lumen was occupied by inflammatory cells and necrotic cell debris, erosion and edema might occur in villous epithelium and edema of some villi; +3 indicated more extensive loss of villous epithelium (up to 50%) with necrosis and inflammation, the remaining villi often were edematous and pale and red blood cells were often packed in capillaries at the base of the epithelium; and +4 indicated extensive loss of villi (>50%), necrosis, and prominent inflammation (usually neutrophils), the lumen was sometimes occluded with debris and inflammatory cells and disruption and inflammation often goes all the way into the crypts with epithelial cell degeneration.

## Detection of the GTD in Toxin-Exposed Intestine by Immunoprecipitation

Whole ligated intestinal lumina were flushed with icy cold PBS 3 times after toxin exposure. Tissues were homogenized in lysis buffer (250 mmol/L sucrose, 100 mmol/L KCl, 1 mmol/L phenylmethylsulfonyl fluoride, and protease inhibitor cocktail; Sigma). The homogenates were lysed further by sonication and freeze-thaw cycles. After lysis, the centrifuged supernatants were pre-incubated with 5D-Fc fusion antibody against the GTD of TcdB.[23] The antibody-GTD complex then was precipitated using Protein A beads. The presence of the GTD on pull-down beads was measured by Western blot with camelid single domain (V$_H$H) monoclonal antibody (clone E3-E-tag[23]) against the GTD of TcdB and horseradish-peroxidase–conjugated goat anti–E-Tag secondary antibody (Bethyl Laboratories, Inc, Montgomery, TX).

## Inositol Hexakisphosphate–Induced Autocleavage of Toxins

All toxin proteins were diluted in 20 mmol/L Tris (pH 8.0) buffer to a concentration of 10 $\mu$g/mL in a final volume of 20 $\mu$L. Autoprocessing was initiated by the addition of inositol hexakisphosphate (InsP$_6$) at the indicated final concentrations. After incubation at room temperature for the indicated times, the reactions were stopped by sodium dodecyl sulfate sample buffer and analyzed by Western blot using monoclonal antibodies against the 2 toxins.

## Human Intestinal Epithelial Monolayer

A human ileocecal colorectal adenocarcinoma cell line (HCT8) from American Type Culture Collection was maintained in RPMI 1640 medium containing 10% fetal bovine serum, 100 U/mL penicillin, 100 $\mu$g/mL streptomycin, 2 mmol/L L-glutamine, and 1 mmol/L sodium pyruvate. HCT8 cells (2 X 10$^4$) were seeded into the apical compartment of a Transwell culture chamber, attached, and grown on the Transwell microporous filter. Cells were cultured for approximately 10 days. On day 1, after attachment, medium in apical and basal compartments was replaced with fresh medium to remove unattached cells. Medium was replaced continuously every other day to supplement nutrition. After approximately 10 to 14 days, when the transepithelial electrical resistance (TER) reached 1200–1500 $\Omega$, the monolayer was established and ready for use. After the application of toxins, the TER was measured at 0, 2, 7, and 24 hours and expressed as a percentage of TER at time 0. The experiments were repeated 3 times, and triplicate wells of monolayers were assayed each time.

## Human 3-Dimensional Organotypic Intestinal Model

The 3-dimensional (3D) bioengineered model of the human intestinal mucosa was established as described previously.[24] It comprised multiples cell types including primary human lymphocytes, fibroblasts, and endothelial cells, as well as HCT8 cells. Briefly, fibroblasts and endothelial cells were embedded in a collagen-I extracellular matrix enriched with additional gut basement membrane proteins. Then, epithelial cells were added to the vessels and cultured under microgravity conditions provided by rotating-wall-vessel bioreactors. After 4 and 9 days ($\pm$1
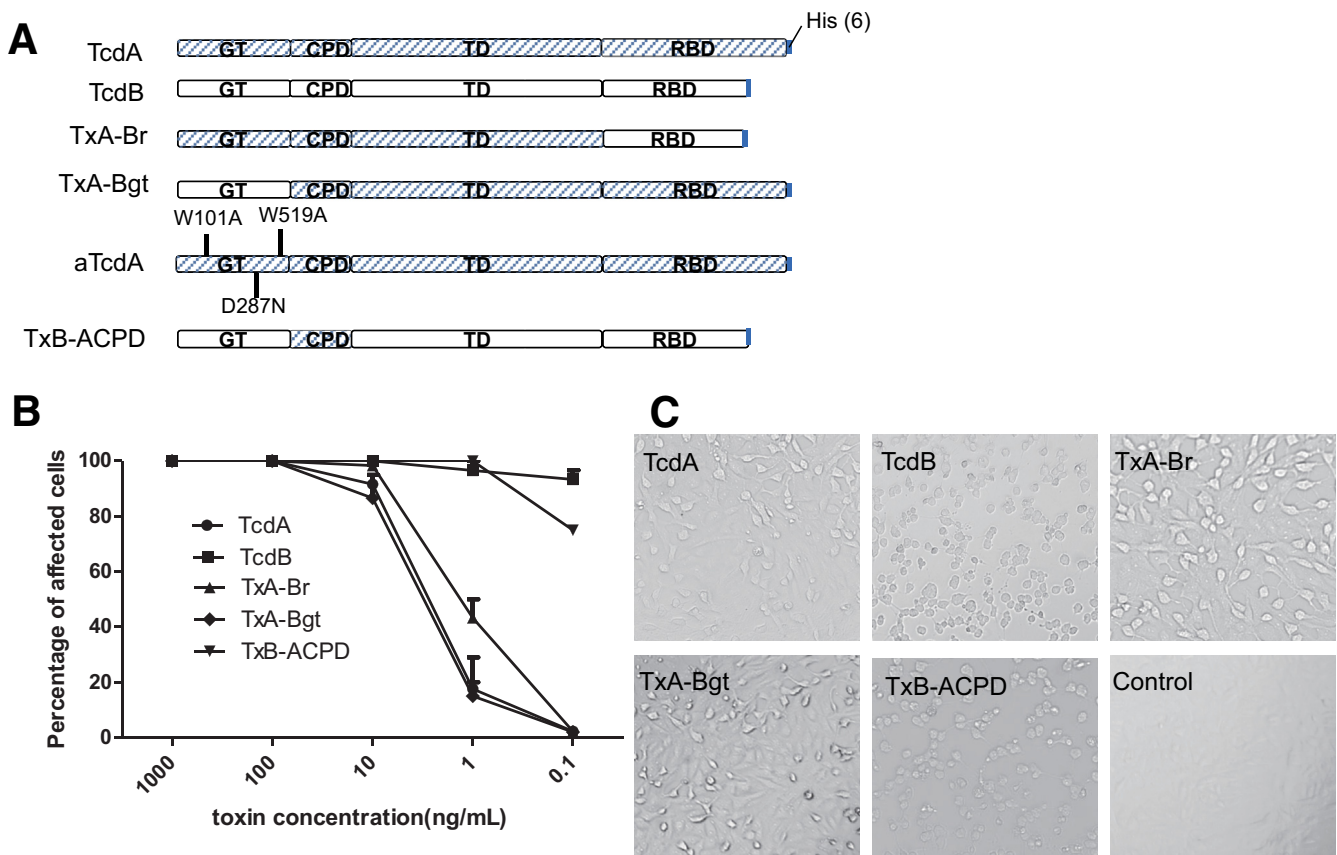


**Figure 1. Cytotoxicity of chimeric toxins on cultured cells.** (*A*) The structure of each chimeric toxin. TxA-Br is TcdA with the RBD from TcdB; TxA-Bgt is TcdA with the GTD from TcdB; aTcdA has 3 point mutations in the GTD abolishing glucosyltransferase function; TxB-ACPD is TcdB with the CPD from TcdA. (*B*) Vero cells were treated with various serially diluted toxins. The percentage of cell rounding was measured after 24 hours of toxin exposure. (*C*) The phase-contrast microscopy images of the cells treated with 1 ng/mL of toxin for 24 hours.

day), the lymphocytes were added to the culture. The epithelial cells in this 3D model consisted of a human adenocarcinoma enterocyte cell line HCT8 that was originally derived from the junction of the small and large

bowel. These epithelial cells did not express either classic or nonclassic HLA-class I molecules. Thus, it allowed the culture of the epithelial cells with peripheral blood mononuclear cells (PBMCs) of different HLA class I haplotypes in
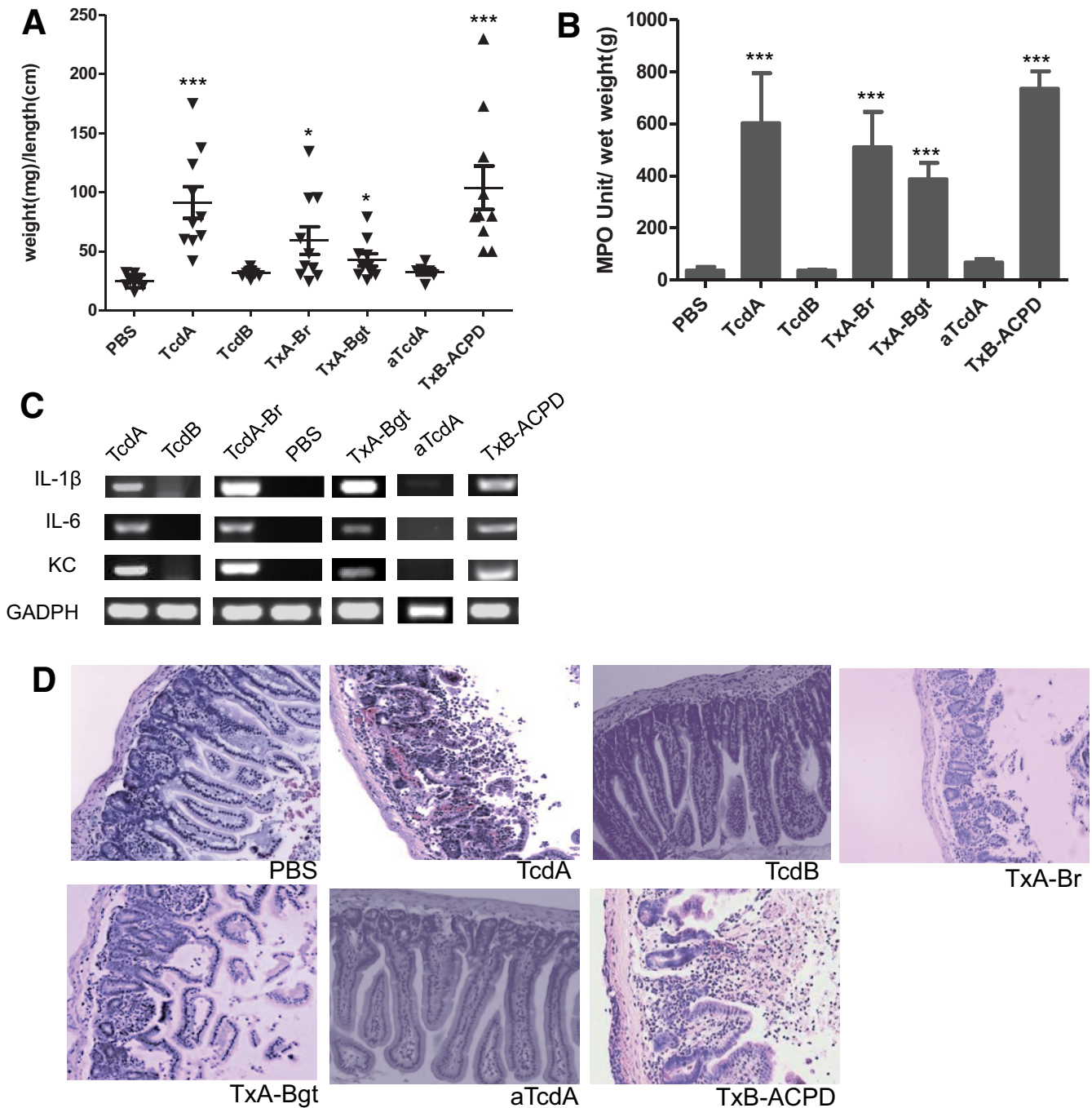


**Figure 2. Induction of acute inflammatory responses by wild-type and chimeric toxins.** TcdA, TcdB, TxA-Br, TxA-Bgt, TxB-ACPD, or vehicle control (PBS) was injected into ligated ileal loops. The mice (n = 10) were killed 4 hours after injection and the ileal loops were collected for subsequent analysis. ***$P$ < .001 (compared with PBS control). (A) Intestinal fluid accumulation was quantitated by the weight-to-length (mg/cm) ratio of the ileal loops. (B) MPO activity of the toxin-treated intestinal tissues. Intestinal tissues were homogenized to extract MPO and MPO activity units were calculated from a standard curve generated using purified MPO. (C) Messenger RNA expression of inflammatory cytokines in ileal tissues after PBS or toxin treatments. Semiquantitative reverse-transcription PCR was performed to detect the expressions of keratinocyte chemoattractant (KC), IL-1$\beta$, and IL-6 messenger RNAs. Equal loading was controlled by the amplification of the housekeeping gene glyceraldehyde-3-phosphate dehydrogenase (GAPDH). (D) Representative H&E-stained sections of treated ilea.
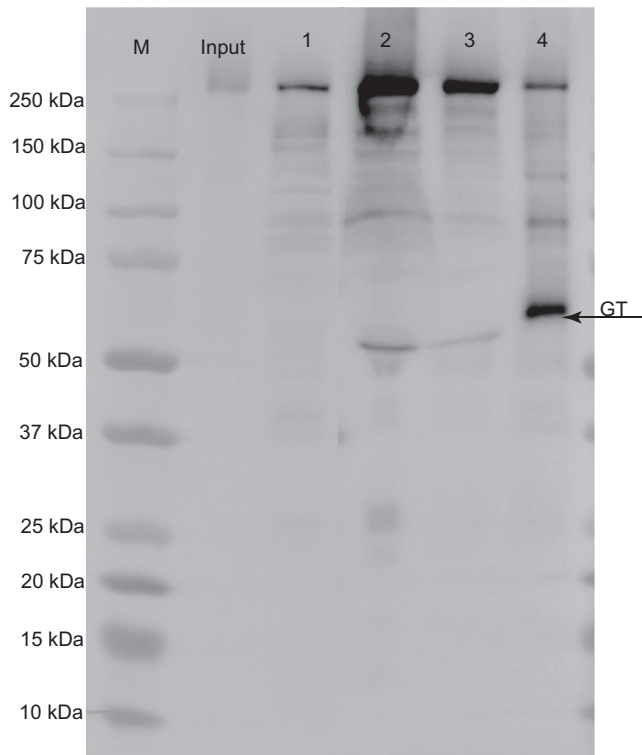
**Figure 3. Detection of TcdB in gut flush.** TcdB was injected into ligated ileal loops and the loops were collected 4 hours later. The gut contents were flushed with PBS and loaded on a sodium dodecyl sulfate–polyacrylamide gel electrophoresis gel. Input was TcdB before injection into the loops; lanes marked 1–3 were gut flush from 3 different ileal loops; and lane 4 was autoprocessed TcdB in the presence of InsP$_6$ as a control. Monoclonal antibody E3 that recognizes the N-terminus of GTD of TcdB was used for detection in Western blot. M, marker.



**Figure 4. Mean histology scores of ilea sections.** Statistical differences between experimental groups and PBS control group were determined by Student $t$ test. *$P < .05$, **$P < .01$, and ***$P < .001$ (compared with PBS control).

the absence of epithelial cell–PBMC alloreactivity. The bioreactors consisted of a rotating vessel with a co-axial oxygenator in the center. The oxygenator rotated concurrently with the outer wall of the vessel, thereby allowing gas transfer while avoiding bubble formation and consequent turbulence. These conditions resulted in laminar flow and minimal shear force that models reduced gravity (microgravity). Consequently, inside the culture vessel, intercellular forces were more evident or more effective in promoting cell differentiation. The experiments were repeated twice, and triplicate wells were assessed for cytokines.

### PBMC Isolation

Human PBMCs were isolated from fresh blood of healthy donors using Ficoll-Paque PLUS (GE Healthcare, Uppsala, Sweden) according to the manufacturer's instructions. PBMCs were frozen in liquid nitrogen at $3 \times 10^6$ cells per vial until use. Vials were rapidly thawed in a 37°C water bath and PBMCs were cultured in RPMI 1640 medium (Invitrogen) containing 10% complement-inactivated fetal bovine serum (Invitrogen) and 100 U/
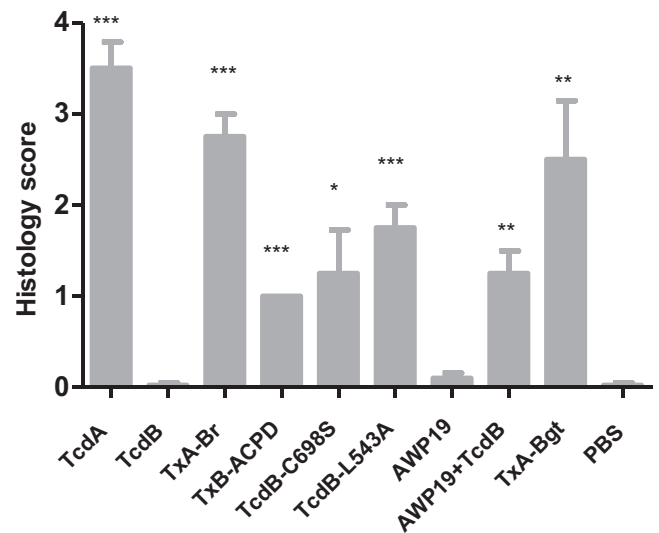
mL of penicillin and 100 $\mu$g/mL of streptomycin (Invitrogen) as described previously.[25] Cell viability was >93% by trypan blue staining. PBMCs were seeded in a 96-well plate at $5 \times 10^4$ cells per well, and cultured with or without TcdA, TcdB, or TcdB-L543A (100 ng/mL) for 24 hours in a 37°C incubator with 5% CO$_2$. PBMCs from 2 healthy donors were used for this assay, and triplicate wells were assessed for cytokines.

### Cytokine Detection

Fresh supernatants from cell or tissue culture were collected and cytokine assays were performed by using human IL-8 enzyme-linked immunosorbent assay (cat. 431507; BioLegend), V-PLEX Cytokine Panel 1 (cat. K15050D; MSD, Rockville, MD), and V-PLEX Proinflammatory Panel 1 Kits according to the manufacturers' instructions (cat. K15050D and K15049D; MSD).

### Statistical Analysis

Data were analyzed by Student $t$ test using the Prism statistical software program (GraphPad Software, Inc, La Jolla, CA). Results are expressed as means ± SEM. The difference between the 2 groups was statistically significant if $P < .05$. No randomization was used in this study.

## Results

### CPD Instead of RBD or GTD Differentiates the Acute Enteric Inflammatory Responses to TcdA and TcdB

To identify the domain that regulates the inflammatory activity of TcdA and TcdB, we constructed functional chimeric toxins TxA-Br, TxA-Bgt, and TxB-ACPD that swapped domains between TcdA and TcdB (Figure 1). We examined the acute inflammatory responses to these
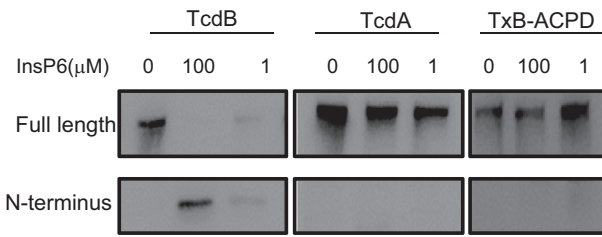
**Figure 5. Autoprocessing of TxB-ACPD. InsP$_6$ triggered autocleavage of wild-type and chimeric toxins.** Wild-type TcdA, TcdB, and TxB-ACPD were exposed to the indicated amounts of InsP$_6$ for 2 hours. Western blot was performed using monoclonal antibodies against the GTD of TcdA or TcdB, respectively.

chimeric toxins in a mouse ileal loop model that clearly differentiates the response to TcdA from the response to TcdB (Figure 2). The lack of enterotoxic response in the ileum induced by TcdB was not caused by proteolytic degradation of TcdB in ilea because TcdB recovered from gut lavage was full-length and cytotoxic (Figure 3 and data not shown). Similar to wild-type TcdA, all chimeras were fully enterotoxic in ligated ilea. Significant intestinal exudate with average weight-to-length ratios ranging from approximately 50 to 100, substantial MPO activity, and high messenger RNA expression of proinflammatory cytokines were observed in chimeric toxin-treated loops (Figure 2A–C). On a microscopic level, the 3 chimeras induced complete disruption of intestinal villi and mucosal architecture in ilea, with considerable neutrophil

influx and necrosis extending into the crypts (Figure 2D), which was consistent with significantly higher histologic scores compared with the PBS group (Figure 4). In addition, a glucosyltransferase-deficient mutant TcdA (aTcdA in Figure 1A), which is nontoxic when applied to cultured cells or injected systemically into mice,[21] failed to induce any observable inflammatory responses or tissue damage in mouse ilea (Figure 2). These data suggested that although the glucosyltransferase activity is required for the enterotoxic responses, the CPD is prominently involved in regulating the acute inflammation caused by the toxins in mice.

## Involvement of CPD Activity in the Enterotoxic Activity of TcdB

The CPDs of the toxins harbor a cysteine protease that mediates the toxins' autoprocessing and releasing of their GTDs in the presence of InsP$_6$. Compared with TcdB, TxB-ACPD and TcdA were less efficient in GTD release in the presence of either 1 or 100 μmol/L of InsP$_6$ (Figure 5). Thus, we hypothesized that the cysteine protease activity of TcdB may be associated with its enterotoxicity. Ligated gut loops injected with cysteine protease-deficient mutant TcdB-C698S[6,20] developed significant fluid accumulation (Figure 6A). The mutant TcdB-C698S, but not its wild type, induced significantly increased MPO activity (Figure 6B) and proinflammatory cytokine responses (Figure 6C). Furthermore, histology analysis showed that TcdB-C698S induced severe edema, neutrophil infiltration, and shortening and/or
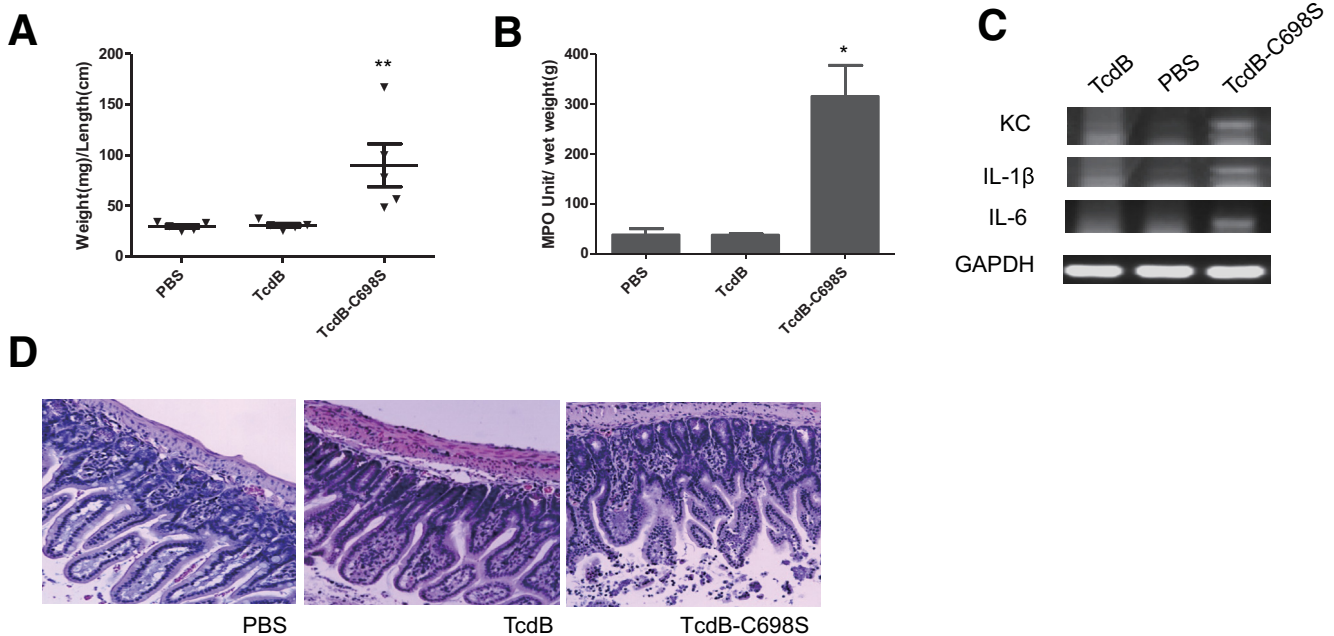


**Figure 6. Induction of acute inflammatory responses by cysteine protease-deficient TcdB-C698S.** TcdB, TcdB-C698S, or PBS was injected into ligated ileal loops. The mice (n = 5) were killed 4 hours after injection and the ileal loops were collected for subsequent analysis. *$P < .05$, and **$P < .01$ (compared with PBS control). Intestinal fluid accumulation quantitated by (A) weight-to-length (mg/cm) ratio of the loops, (B) MPO activity, (C) messenger RNA expression of inflammatory cytokines by reverse-transcription PCR, and (D) H&E-stained intestinal tissue sections are shown. GAPDH, glyceraldehyde-3-phosphate dehydrogenase.

damage of villi in the intestines (Figure 6D). The histopathologic changes of TcdB-C698S–treated gut, as quantitated by histology scoring, were significantly greater than TcdB and PBS controls (Figure 4). Although TcdB-C698S lost its cysteine protease activity and became less cytotoxic when compared with wild type,[6,20] it gained new function, becoming more inflammatory.

To further confirm the role of CPD in enterotoxic activities, we used chemical inhibitor/substrate analog AWP19 that blocked CPD-mediated autoprocessing. AWP19 and its nonfluorescent form binds to wild-type TcdB in a dose- and time-dependent manner.[22] AWP19 was able to inhibit the release of GTD from TcdB after their co-injection into mouse ileum, as determined by immunoprecipitation of GTD from the toxin-exposed intestinal tissues (Figure 7A). In the presence of CPD chemical inhibitor, the full-length TcdB was not dramatically detected in the tissue lysis supernatant (Figure 7A). The possible reason is that the majority of full-length TcdB, upon binding the inhibitor, might be trapped in the endosome fraction and tethered on the membrane.[23] TcdB showed potent enterotoxic activity in the presence of AWP19 whereas neither AWP19 nor TcdB alone induced any observable fluid secretory responses in the ilea

(Figure 7B). In the presence of the inhibitor, wild-type TcdB induced significant neutrophil infiltration as measured by MPO activity (Figure 7C). Proinflammatory cytokines were up-regulated when the gut was treated with a combination of TcdB and AWP19 (Figure 7D). Atrophied, blunt villi were observed in ileal tissue sections treated with TcdB in the presence of the inhibitor. Extensive edema occurred to villi, resulting in empty epithelia. The area around the lymphoid nodule also showed hemorrhage and cell necrosis (Figure 7E). Consistent with the MPO activity assay, numerous neutrophils infiltrated into intestinal lumen in ilea exposed to TcdB in the presence of the inhibitor, whereas the inhibitor alone and TcdB-alone groups showed normal intestinal structure without neutrophil infiltration (Figures 7C and E and 4). Therefore, the cysteine protease-specific inhibitor AWP19 potentiated TcdB enterotoxic activity and consequently induced severe ileitis in mice.

## Autoprocessing of the TcdB Regulates Its Enterotoxic Activity

To further understand the mechanism regulating enteric responses to the toxin, we used a noncleavable TcdB mutant
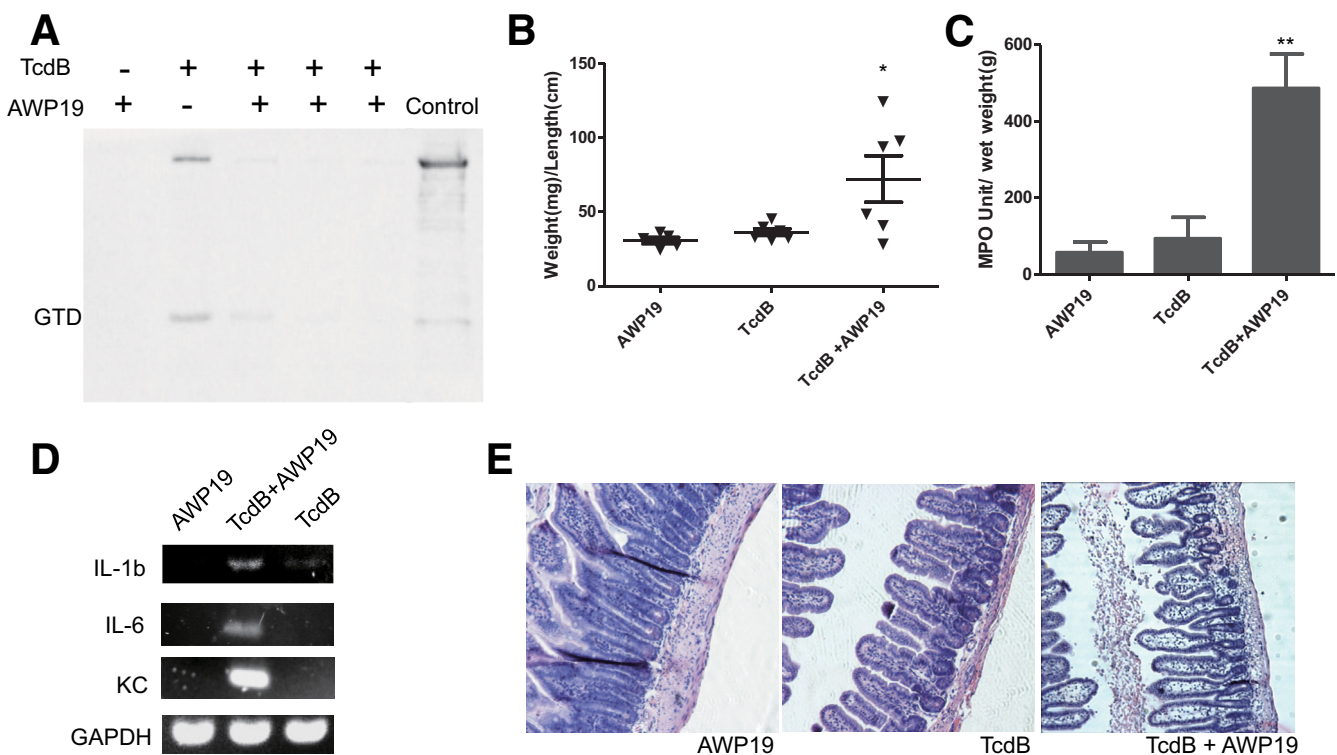


**Figure 7. Induction of acute inflammatory responses by wild-type TcdB in the presence of a cysteine protease inhibitor.** TcdB with or without AWP19, or AWP19 alone was injected into ligated ileal loops. The mice (n = 6) were killed and the ileal loops were collected for subsequent analysis. (A) Immunoprecipitation of the GTD fragment in tissue lysates. Mouse ligated ileal loops were injected with TcdB alone or TcdB in the presence of AWP19 and the intestinal tissues were collected 4 hours later for the immunoprecipitation assay. Samples from 3 different mice treated with TcdB together with AWP19 were shown. Wild-type TcdB pretreated with InsP$_6$ was loaded as an immunoblotting control. (B–E) Analysis of ileal loops by (B) quantitation of intestinal fluid accumulation by weight-to-length ratio, (C) MPO activity, (D) messenger RNA expression of inflammatory cytokines by reverse-transcription PCR, and (E) H&E-stained intestinal tissue sections are shown. *P < .05, **P < .01 (compared with PBS control). GAPDH, glyceraldehyde-3-phosphate dehydrogenase; KC, keratinocyte chemoattractant.

TcdB-L543A to determine whether cysteine protease activity or autoprocessing is involved in regulating the enterotoxic effects. TcdB-L543A has an intact cysteine protease domain but is unable to undergo autoprocessing and release of the GTD fragment in response to InsP$_6$ treatment.[6] The point mutation did not affect its cysteine protease activity because it bound AWP19 in the presence of InsP$_6$ (Figure 8). TcdB-L543A–treated gut loops showed dramatic fluid accumulation, with an average weight-to-length value of approximately 100 mg/cm (Figure 9A). Significantly increased MPO activity and enhanced production of proinflammatory cytokines were detected in TcdB-L543A–exposed tissues (Figure 9B and C). Histopathologic examination of TcdB-L543A loops showed inflamed intestinal epithelia with swollen and damaged villi, and neutrophil influx (Figure 9D). The histology score of TcdB-L543A–treated tissues was markedly higher than that of TcdB or PBS-treated tissues (Figure 4). These data show that toxin autoprocessing, rather than cysteine protease activity, is critical for regulating the inflammatory response of TcdB in mouse ilea.

### Noncleavable TcdB-L543A Is More Proinflammatory in Human Intestinal Tissues Than Wild-Type TcdB

Next, we examined whether the observations in the mouse model were consistent in human tissues, such as colonocytes and intestinal organoids. Because IL-8 is a major proinflammatory cytokine produced by intestinal epithelial cells in response to *C difficile* toxins,[26–29] we first evaluated the IL-8 production by polarized human colonocyte cell line HCT8 in Transwells. Although the reduction of TER of the monolayer was comparable between TcdB-L543A and TcdB (Figure 10), the mutant was significantly more potent in inducing the expression of IL-8. HCT8 monolayers treated with TcdB-L543A or TcdA secreted twice as much IL-8 than TcdB-treated monolayers (Figure 11A). We then evaluated IL-8 production in intestinal organoids.

Cultured human 3D intestinal organoids were previously reported to be structural and functional organotypic models with multiple cell types including lymphocytes and differentiated lineages of goblet and M cells.[24] TcdB-L543A was significantly more potent than wild-type TcdB in the induction of IL-8 by the intestinal organoids, although the level was lower than that from TcdA-treated tissues (Figure 11B). In addition to IL-8, the noncleavable mutant TcdB-L543A induced higher expression of other proinflammatory cytokines, such as IL-6, tumor necrosis factor-$\alpha$, and IL-1$\beta$, than TcdB in 3D organoids (Figure 12).

### The Noncleavable TcdB-L543A Induces Human PBMCs to Produce Proinflammatory Cytokines

Because immune cells likely contribute to the pathogenesis of CDI by producing cytokines/chemokine once they encounter toxins that have passed through damaged intestinal epithelia into the submucosal and systemic circulation, we examined the cytokine production of human PMBCs in response to the autoprocessing-deficient TcdB mutant. In comparison with TcdB, TcdB-L543A more potently induced 11 cytokines in PBMCs of the 20 cytokines tested, including IL-12p70, IL-13, IL-1$\beta$, IL-4, IL-6, IL-8, IL-7, IL-1$\alpha$, IL-17, tumor necrosis factor-$\alpha$, and IL5 (Figures 13 and 14). Therefore, the autoprocessing-deficient mutant TcdB-L543A was more proinflammatory than wild-type TcdB in human immune cells.

## Discussion

The functions of the domains in regulating cytotoxicity of the 2 toxins have been studied extensively,[6,7,22,30,31] however, the underlying mechanism that regulates the proinflammatory activity of TcdA and TcdB remains elusive. Earlier studies using ligated ileal loop models and more recent studies using cecum or intrarectal toxin instillation



**Figure 8. Binding of AWP19 to TcdB-L543A in the presence of InsP$_6$.** TcdB or TcdB-L543A (0.1 $\mu$g/$\mu$L) was incubated with the indicated doses of AWP19 (labeled with TAMRA) in 25 $\mu$mol/L InsP$_6$, in 20 $\mu$mol/L Tris buffer (pH 8.0), at 37°C for 1 hour. The reactions were resolved by sodium dodecyl sulfate–polyacrylamide gel electrophoresis. (A) Fluorescence was measured using the G-Box Chemi system (Synoptics Ltd, Cambridge, UK). (B) To show equal loading, proteins then were visualized on the gel by blue staining. TAMRA, carboxytetramethylrhodamine.
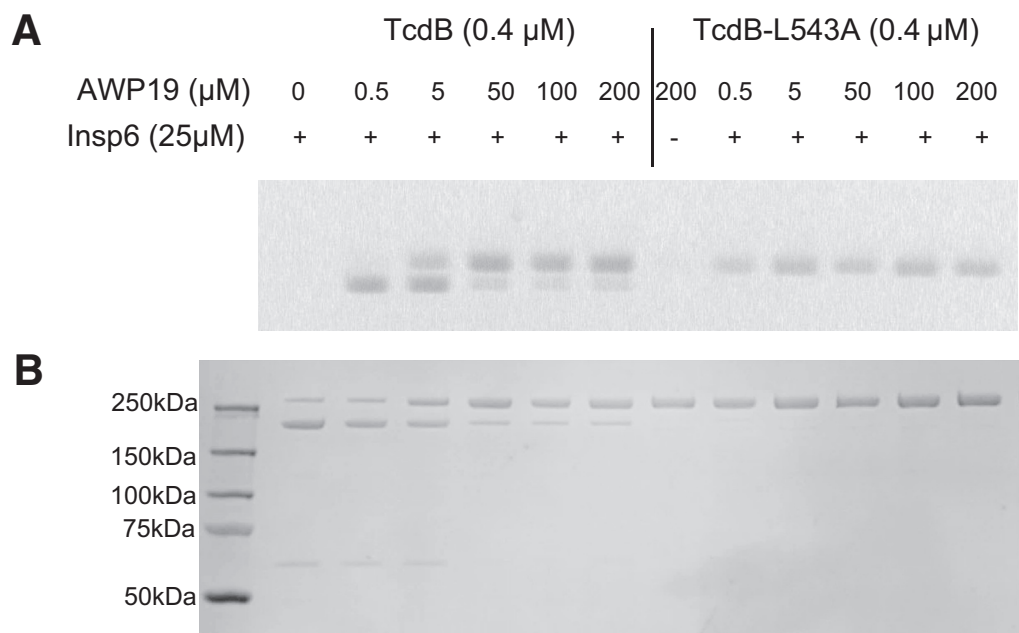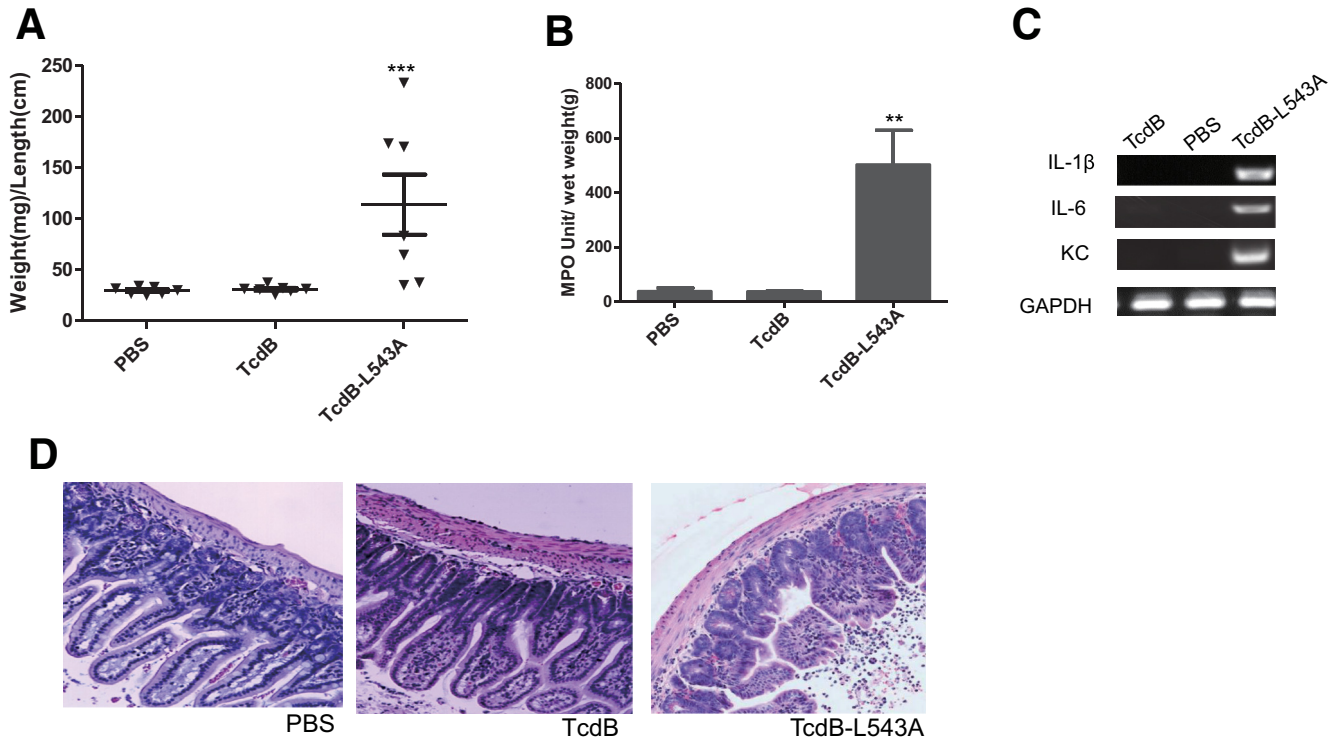
**Figure 9. Induction of acute inflammatory responses by noncleavable TcdB-L543A.** TcdB, TcdB-L543A, or PBS was injected into ligated ileal loops. The mice (n = 7) were killed 4 hours after injection and the ileal loops were collected for subsequent analysis. ***$P$ < .001 (compared with PBS control). Intestinal fluid accumulation was quantitated by (*A*) weight-to-length (mg/cm) ratio of the loops, (*B*) MPO activity, (*C*) messenger RNA expression of inflammatory cytokines by reverse-transcription PCR, and (*D*) H&E-stained intestinal tissue sections are shown. GAPDH, glyceraldehyde-3-phosphate dehydrogenase; KC, keratinocyte chemoattractant.

have consistently shown that TcdA, but not TcdB, induced rapid enterotoxic responses resembling some characteristics of human CDI in multiple animal models.[10–12,14,19,32–36] The molecular mechanism that governs such a differential response is unknown, but several reports have shown that the expression and distribution of toxin receptors on target cells[37,38] and host intestinal epithelia[33] may account for the different responses of the host to the 2 toxins. However, in this study, we found that swapping TcdA's RBD for that of TcdB did not quell inflammation, but, more importantly, a single point mutation in the CPD or in the cysteine autocleavage site of TcdB (TcdB-C698S and TcdB-L543A, respectively) significantly enhanced the toxin's proinflammatory activity. Moreover, chemical inhibition of TcdB autoprocessing converted wild-type TcdB into a proinflammatory enterotoxin in a mouse ileal loop model. These results indicated that the receptor binding of the toxins to host intestinal epithelia did not differentiate the inflammatory activities of the toxins because these point mutations within CPD and the chemicals are unlikely to affect TcdB-receptor binding activity. In addition to receptor binding, we examined glucosyltransferase (GT) activity. TcdB possesses a more potent GT than that of TcdA, which contributes to its stronger cytotoxicity.[30] The acute intestinal inflammatory responses induced by TcdA were dependent on the toxin's GT activity because GT-deficient aTcdA failed to induce any measurable responses. However, the disparate potency in GT

activity between the 2 toxins cannot explain their difference in proinflammatory activity because the TxA-Bgt and TxB-ACPD chimeras that harbor GTD from TcdB were enterotoxigenic. These data indicated that neither the receptor interaction of the toxins with host intestinal epithelia nor the GT activity is
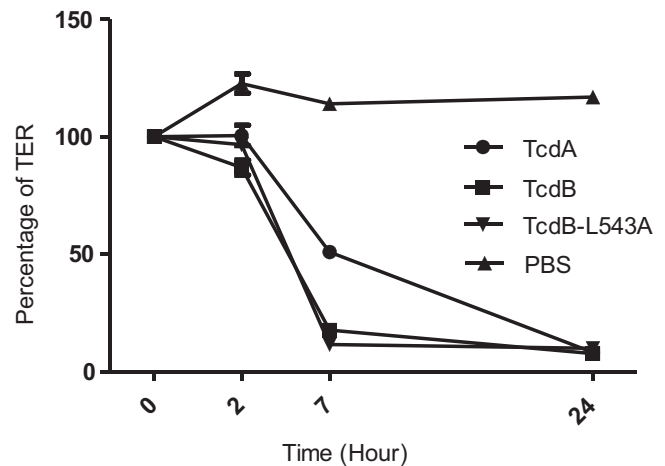


**Figure 10. TER change of HCT8 monolayers after toxin exposure.** HCT8 monolayers were exposed to 100 ng/mL of TcdA, TcdB, or TcdB-L543A. TER was measured at the indicated time points.
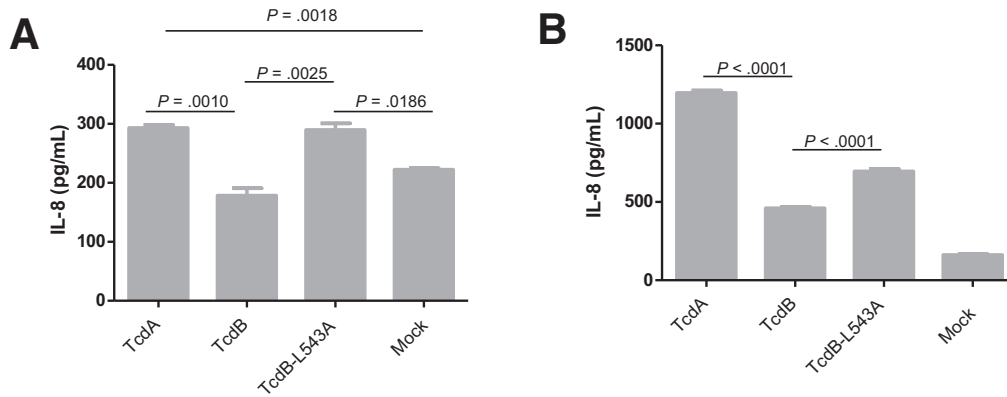
**Figure 11. IL-8 induction by human colonic monolayer and 3D colonic tissues after exposure to toxins.** (*A*) HCT8 monolayers cultured in Transwells were exposed to 100 ng/mL of TcdA, TcdB, or TcdB-L543A for 24 hours. The culture supernatants were collected to detect IL-8 production by enzyme-linked immunosorbent assay. (*B*) Human intestinal 3D cultured organs were exposed to 1000 ng/mL of TcdA, TcdB, or TcdB-L543A for 24 hours. The culture supernatants were collected for enzyme-linked immunosorbent assay to detect IL-8 production.

likely the major factor that differentiates toxin-induced inflammatory responses.

Instead of receptor interaction or GT activity, we focused on the CPD and autoprocessing. The CPDs from the 2 toxins are highly homologous[39]: each cysteine protease targets an intramolecular substrate and mediates $InsP_6$-induced autoprocessing to release the GTD into host cytosol.[40,41] However, TcdB is more susceptible to $InsP_6$-induced autocleavage than wild-type TcdA.[7,39] The cleaved GTD fragment from TcdB-intoxicated cells is readily identifiable,[6,42,43] whereas autocleavage of TcdA in host cells has not yet been identified. Therefore, we used TcdB in which CPD-mediated autoprocessing can be readily manipulated through mutagenesis or with chemical inhibitors. TcdB mutations at the CPD catalytic triad (TcdB-C698S) or autocleavage site (TcdB-L543A), or chemical inhibition of autoprocessing, blocked the release of the GTD and reduced the cytotoxicity of the toxin,[6,20,22,44] yet significantly enhanced the toxin's ability to stimulate acute inflammatory responses in mouse intestine. The noncleavable mutant
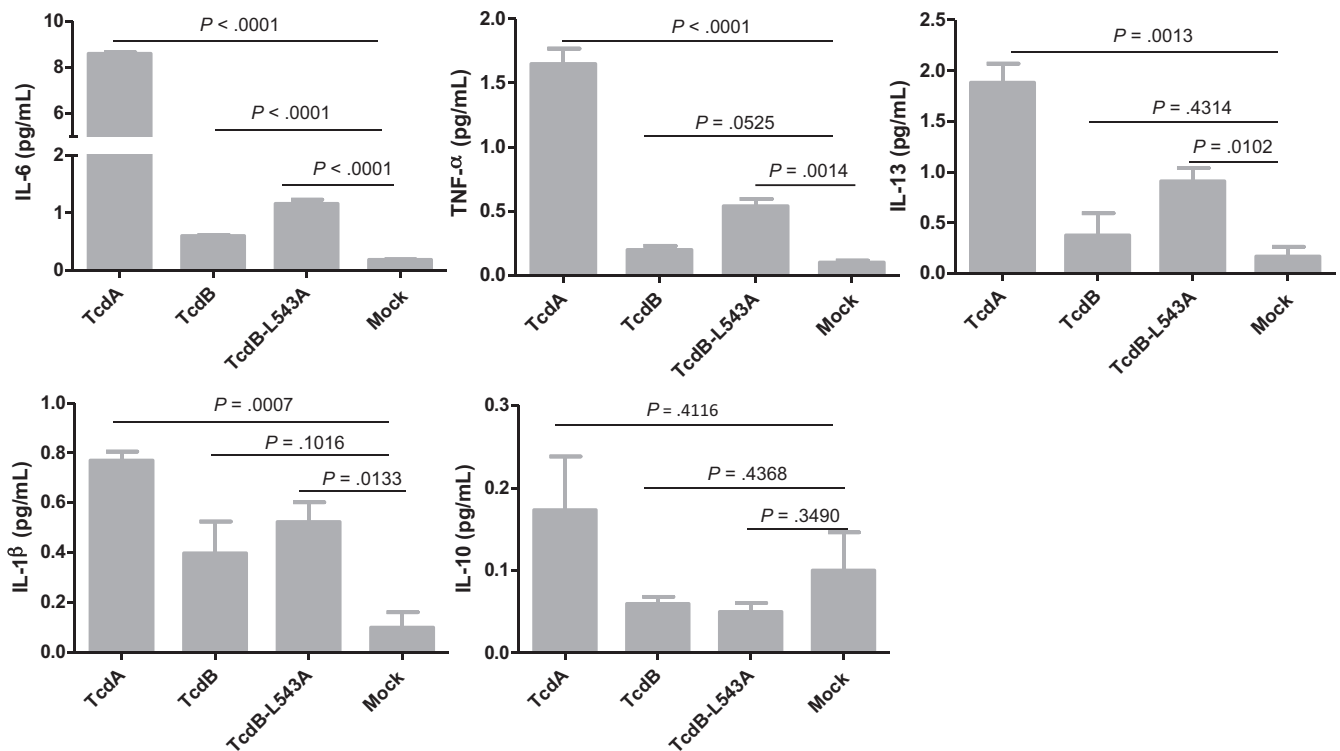


**Figure 12. Proinflammatory cytokines produced by 3D colonic tissues after exposure to toxins.** Human intestinal 3D cultured organs were exposed to 1000 ng/mL of TcdA, TcdB, or TcdB-L543A for 24 hours. The culture supernatants were collected and assayed to detect cytokine production.
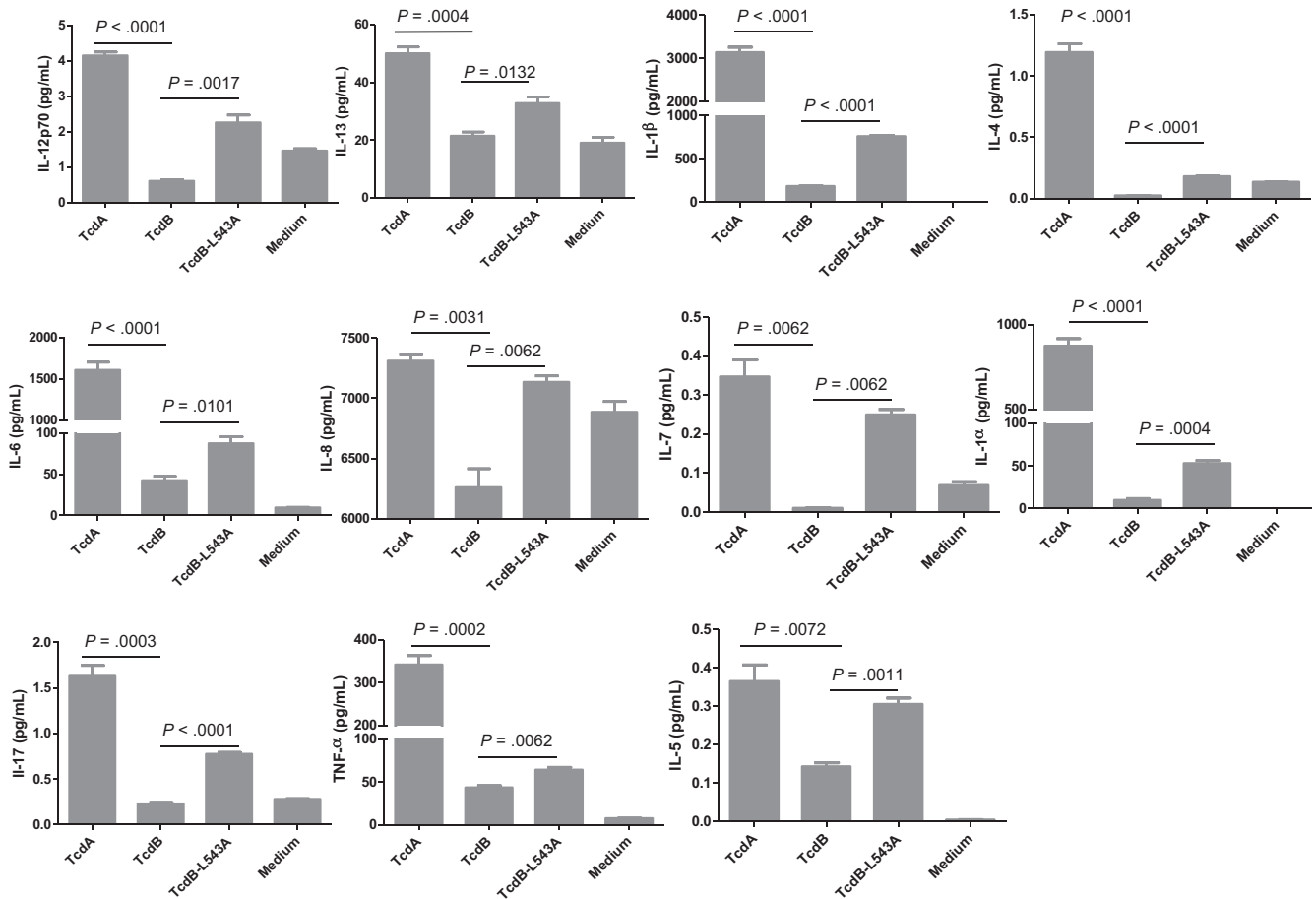
**Figure 13. Production of proinflammatory cytokines by human PBMCs.** Human PBMCs were incubated with 100 ng/mL of TcdA, TcdB, or TcdB-L543A for 24 hours. The culture supernatants were collected for cytokine assays using the V-PLEX Cytokine Panel 1 and Proinflammatory Panel 1 Kits.

TcdB-L543A, with an intact functional CPD, showed significantly higher inflammatory activity than wild-type TcdB in both human intestinal tissues and immune cells, and also in animal intestines, showing that it is the autoprocessing, rather than the intrinsic cysteine protease activity of the toxins, that regulates the toxins' proinflammatory activities. It also is possible that the products of autoprocessing regulate the inflammatory responses. The enhanced proinflammatory activity of TcdB-L543A is not likely owing to structural alteration of the toxin because a chemical inhibitor of the cysteine protease that blocks TcdB autoprocessing[22,45] converted wild-type TcdB into a potent enterotoxin in murine ileal loops, possibly keeping the full-length toxin bound to the endosome membrane. Thus, data presented in this work showed an unexpected function of CPD: regulation of the proinflammatory activity of *C difficile* glucosylating toxins. Because CPD activity clearly is associated with cytotoxicity,[6,7,22,46] CPD-mediated autoprocessing of the toxins may act as a fine tuner of their biological activities, in that it positively regulates toxins' cytotoxicity, but negatively regulates their acute proinflammatory activity.

Clinical studies analyzing various biomarkers of CDI patients show the strong relationships between intestinal inflammation and clinical disease severity and outcome.[8,47–49] Recently, Yacyshyn et al[49] found that a proinflammatory PBMC phenotype in patients correlated with CDI recurrence, indicating a critical role of immune cells in response to *C difficile* infection. Our data showed that IL-8, a potent chemokine that recruits neutrophils, was the dominant cytokine produced by human colonic tissues in response to *C difficile* toxin treatment. The noncleavable mutant TcdB-L543A, when compared with wild-type TcdB, significantly up-regulated the production of several proinflammatory cytokines in human intestinal tissues as well as human PBMCs, suggesting that the autoprocessing of the toxins also may regulate the inflammatory response during CDI manifestation in human beings.

Isogenic or clinical *C difficile* TcdA⁻B⁺ strains were able to infect hamsters and mice and induce similar disease symptoms as those caused by TcdA⁺B⁺ strains,[13,15,50–52] suggesting that TcdB, either independently or together with other bacterial factors, causes intestinal inflammatory disease in animals. Thus, TcdB is still an essential virulence factor of CDI, although it fails to stimulate dramatic inflammation in the murine gut loop model within 4 hours of exposure. Recently, studies using cecum or intrarectal toxin instillation showed that TcdB alone induced colitis, although in a significantly slower fashion than TcdA.[19,35,36]
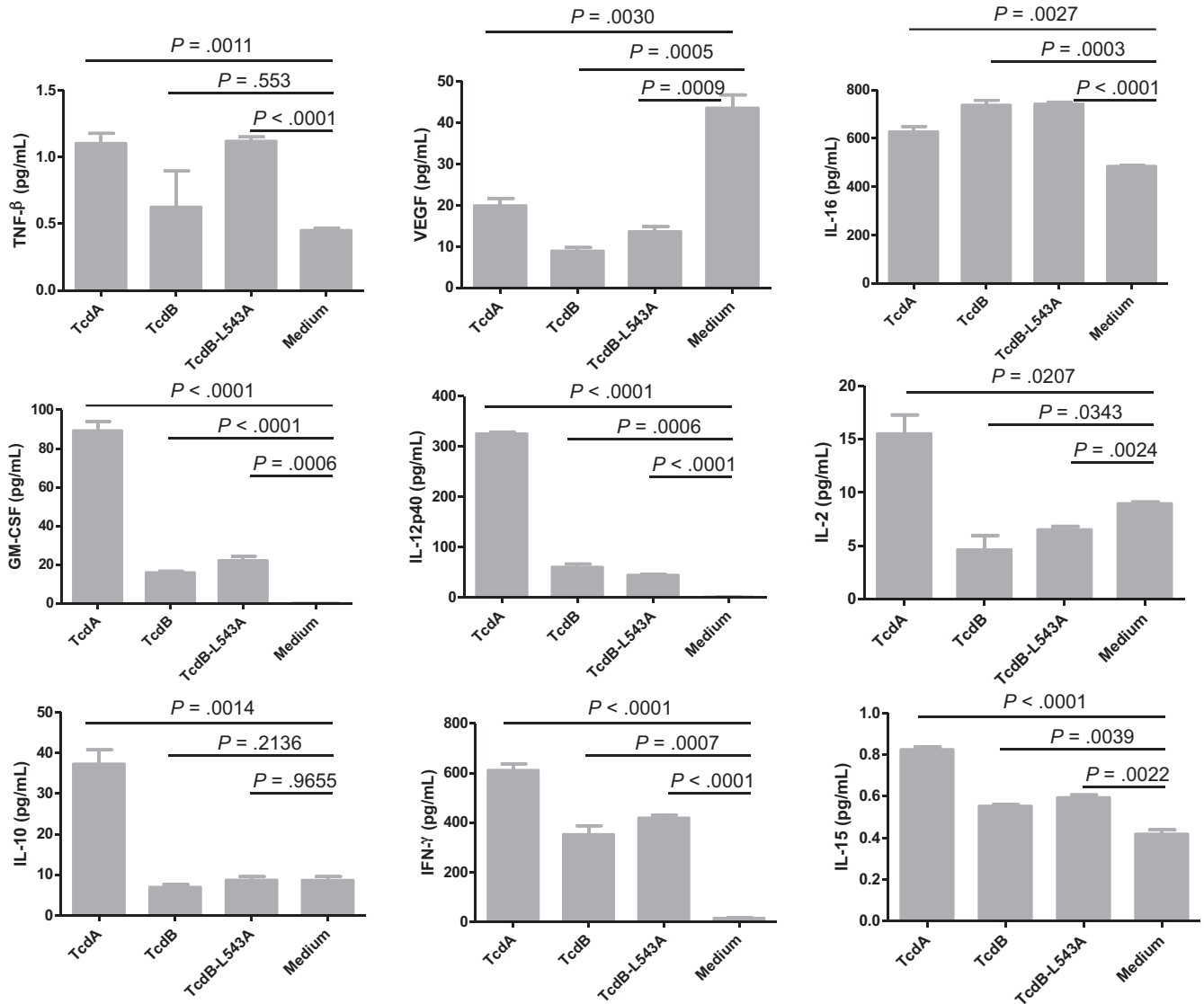
**Figure 14. Cytokines produced by human PBMCs after exposure to toxins.** Human PBMCs were exposed to 100 ng/mL of TcdA, TcdB, or TcdB-L543A for 24 hours. The culture supernatants were collected and assayed to detect cytokine expression.

Thus, the delayed intestinal inflammation induced by purified TcdB may be caused by GT-dependent cytotoxicity of epithelial cells, which in turn generates more tissue damage. It is likely that the pathogenesis of CDI is mediated at least by both the cytotoxic and proinflammatory activities of the 2 toxins and the disease outcomes may be affected by the potency of these biological activities. Savidge et al[20] and Bender et al[53] reported that treatment of animals with CPD inhibitors led to the reduction of overall severity of CDI. It is possible that early intestinal inflammatory responses, augmented by using CPD inhibitors, are protective against severe outcomes of CDI. Whether or not an inflammatory response becomes pathogenic, leading to severe CDI, ultimately may be dependent on the potency as well as the kinetics of the response. In fact, a follow-up study by Beilhartz et al[54] showed that the treatment efficacy of ebselen against TcdB may not be by inhibition of autoprocessing but by preventing GTD mediated effects. Nevertheless, our data

indicated that a therapeutic approach of directly targeting cysteine protease activities may not be an optimal strategy.

In summary, our data show a novel mechanism: CPD-mediated autoprocessing of *C difficile* toxins regulates their proinflammatory activities. Thus, our study provides a new understanding of the molecular mechanisms of the pathogenesis of *C difficile* toxins and insights into designing new therapeutics against CDI.

## References

1. Kelly CP, LaMont JT. Clostridium difficile - more difficult than ever. N Engl J Med 2008;359:1932–1940.
2. Voth DE, Ballard JD. Clostridium difficile toxins: mechanism of action and role in disease. Clin Microbiol Rev 2005;18:247–263.
3. Jank T, Aktories K. Structure and mode of action of clostridial glucosylating toxins: the ABCD model. Trends Microbiol 2008;16:222–229.

4. Yuan P, Zhang H, Cai C, Zhu S, Zhou Y, Yang X, He R, Li C, Guo S, Li S, Huang T, Perez-Cordon G, Feng H, Wei W. Chondroitin sulfate proteoglycan 4 functions as the cellular receptor for Clostridium difficile toxin B. Cell Res 2015;25:157–168.

5. Tao L, Zhang J, Meraner P, Tovaglieri A, Wu X, Gerhard R, Zhang X, Stallcup WB, Miao J, He X, Hurdle JG, Breault DT, Brass AL, Dong M. Frizzled proteins are colonic epithelial receptors for C. difficile toxin B. Nature 2016;538:350–355.

6. Li S, Shi L, Yang Z, Feng H. Cytotoxicity of Clostridium difficile toxin B does not require cysteine protease-mediated autocleavage and release of the glucosyltransferase domain into the host cell cytosol. Pathog Dis 2013;67:11–18.

7. Kreimeyer I, Euler F, Marckscheffel A, Tatge H, Pich A, Olling A, Schwarz J, Just I, Gerhard R. Autoproteolytic cleavage mediates cytotoxicity of Clostridium difficile toxin A. Naunyn Schmiedebergs Arch Pharmacol 2011; 383:253–262.

8. El Feghaly RE, Bangar H, Haslam DB. The molecular basis of Clostridium difficile disease and host response. Curr Opin Gastroenterol 2015;31:24–29.

9. Lima AA, Lyerly DM, Wilkins TD, Innes DJ, Guerrant RL. Effects of Clostridium difficile toxins A and B in rabbit small and large intestine in vivo and on cultured cells in vitro. Infect Immun 1988;56:582–588.

10. Lyerly DM, Saum KE, MacDonald DK, Wilkins TD. Effects of Clostridium difficile toxins given intragastrically to animals. Infect Immun 1985;47:349–352.

11. Mitchell TJ, Ketley JM, Haslam SC, Stephen J, Burdon DW, Candy DC, Daniel R. Effect of toxin A and B of Clostridium difficile on rabbit ileum and colon. Gut 1986;27:78–85.

12. Triadafilopoulos G, Pothoulakis C, O'Brien MJ, LaMont JT. Differential effects of Clostridium difficile toxins A and B on rabbit ileum. Gastroenterology 1987;93:273–279.

13. Carter GP, Chakravorty A, Pham Nguyen TA, Mileto S, Schreiber F, Li L, Howarth P, Clare S, Cunningham B, Sambol SP, Cheknis A, Figueroa I, Johnson S, Gerding D, Rood JI, Dougan G, Lawley TD, Lyras D. Defining the roles of TcdA and TcdB in localized gastrointestinal disease, systemic organ damage, and the host response during Clostridium difficile infections. mBio 2015;6:e00551.

14. Kuehne SA, Cartman ST, Minton NP. Both, toxin A and toxin B, are important in Clostridium difficile infection. Gut Microbes 2011;2:252–255.

15. Lyras D, O'Connor JR, Howarth PM, Sambol SP, Carter GP, Phumoonna T, Poon R, Adams V, Vedantam G, Johnson S, Gerding DN, Rood JI. Toxin B is essential for virulence of Clostridium difficile. Nature 2009;458:1176–1179.

16. Lonnroth I, Lange S. Toxin A of Clostridium difficile: production, purification and effect in mouse intestine. Acta Pathol Microbiol Immunol Scand B 1983;91:395–400.

17. Libby JM, Wilkins TD. Production of antitoxins to two toxins of Clostridium difficile and immunological comparison of the toxins by cross-neutralization studies. Infect Immun 1982;35:374–376.

18. Just I, Gerhard R. Large clostridial cytotoxins. Rev Physiol Biochem Pharmacol 2004;152:23–47.

19. D'Auria KM, Kolling GL, Donato GM, Warren CA, Gray MC, Hewlett EL, Papin JA. In vivo physiological and transcriptional profiling reveals host responses to Clostridium difficile toxin A and toxin B. Infect Immun 2013; 81:3814–3824.

20. Savidge TC, Urvil P, Oezguen N, Ali K, Choudhury A, Acharya V, Pinchuk I, Torres AG, English RD, Wiktorowicz JE, Loeffelholz M, Kumar R, Shi L, Nie W, Braun W, Herman B, Hausladen A, Feng H, Stamler JS, Pothoulakis C. Host S-nitrosylation inhibits clostridial small molecule-activated glucosylating toxins. Nat Med 2011;17:1136–1141.

21. Wang H, Sun X, Zhang Y, Li S, Chen K, Shi L, Nie W, Kumar R, Tzipori S, Wang J, Savidge T, Feng H. A chimeric toxin vaccine protects against primary and recurrent Clostridium difficile infection. Infect Immun 2012;80:2678–2688.

22. Lanis JM, Hightower LD, Shen A, Ballard JD. TcdB from hypervirulent Clostridium difficile exhibits increased efficiency of autoprocessing. Mol Microbiol 2012;84:66–76.

23. Li S, Shi L, Yang Z, Zhang Y, Perez-Cordon G, Huang T, Ramsey J, Oezguen N, Savidge TC, Feng H. Critical roles of Clostridium difficile toxin B enzymatic activities in pathogenesis. Infect Immun 2015;83:502–513.

24. Salerno-Goncalves R, Fasano A, Sztein MB. Engineering of a multicellular organotypic model of the human intestinal mucosa. Gastroenterology 2011;141:e18–e20.

25. Akerlund T, Persson I, Unemo M, Noren T, Svenungsson B, Wullt M, Burman LG. Increased sporulation rate of epidemic Clostridium difficile type 027/NAP1. J Clin Microbiol 2008;46:1530–1533.

26. Bobo LD, El Feghaly RE, Chen YS, Dubberke ER, Han Z, Baker AH, Li J, Burnham CA, Haslam DB. MAPK-activated protein kinase 2 contributes to Clostridium difficile-associated inflammation. Infect Immun 2013;81:713–722.

27. Hansen A, Alston L, Tulk SE, Schenck LP, Grassie ME, Alhassan BF, Veermalla AT, Al-Bashir S, Gendron FP, Altier C, MacDonald JA, Beck PL, Hirota SA. The P2Y6 receptor mediates Clostridium difficile toxin-induced CXCL8/IL-8 production and intestinal epithelial barrier dysfunction. PLoS One 2013;8:e81491.

28. Kim JM, Lee JY, Yoon YM, Oh YK, Youn J, Kim YJ. NF-kappa B activation pathway is essential for the chemokine expression in intestinal epithelial cells stimulated with Clostridium difficile toxin A. Scand J Immunol 2006;63:453–460.

29. Na X, Zhao D, Koon HW, Kim H, Husmark J, Moyer MP, Pothoulakis C, LaMont JT. Clostridium difficile toxin B activates the EGF receptor and the ERK/MAP kinase pathway in human colonocytes. Gastroenterology 2005; 128:1002–1011.

30. Chaves-Olarte E, Weidmann M, Eichel-Streiber C, Thelestam M. Toxins A and B from Clostridium difficile differ with respect to enzymatic potencies, cellular substrate specificities, and surface binding to cultured cells. J Clin Invest 1997;100:1734–1741.

31. Lanis JM, Heinlen LD, James JA, Ballard JD. Clostridium difficile 027/BI/NAP1 encodes a hypertoxic and antigenically variable form of TcdB. PLoS Pathog 2013; 9:e1003523.

32. Lyerly DM, Lockwood DE, Richardson SH, Wilkins TD. Biological activities of toxins A and B of Clostridium difficile. Infect Immun 1982;35:1147–1150.

33. Keel MK, Songer JG. The distribution and density of Clostridium difficile toxin receptors on the intestinal mucosa of neonatal pigs. Vet Pathol 2007;44:814–822.

34. Carter GP, Rood JI, Lyras D. The role of toxin A and toxin B in the virulence of Clostridium difficile. Trends Microbiol 2012;20:21–29.

35. Hirota SA, Iablokov V, Tulk SE, Schenck LP, Becker H, Nguyen J, Al Bashir S, Dingle TC, Laing A, Liu J, Li Y, Bolstad J, Mulvey GL, Armstrong GD, MacNaughton WK, Muruve DA, MacDonald JA, Beck PL. Intrarectal instillation of Clostridium difficile toxin A triggers colonic inflammation and tissue damage: development of a novel and efficient mouse model of Clostridium difficile toxin exposure. Infect Immun 2012;80:4474–4484.

36. Yang Z, Zhang Y, Huang T, Feng H. Glucosyltransferase activity of Clostridium difficile toxin B is essential for disease pathogenesis. Gut Microbes 2015;6:221–224.

37. Thelestam M, Chaves-Olarte E. Cytotoxic effects of the Clostridium difficile toxins. Curr Top Microbiol Immunol 2000;250:85–96.

38. Na X, Kim H, Moyer MP, Pothoulakis C, LaMont JT. gp96 is a human colonocyte plasma membrane binding protein for Clostridium difficile toxin A. Infect Immun 2008; 76:2862–2871.

39. Pruitt RN, Chagot B, Cover M, Chazin WJ, Spiller B, Lacy DB. Structure-function analysis of inositol hexakisphosphate-induced autoprocessing in Clostridium difficile toxin A. J Biol Chem 2009; 284:21934–21940.

40. Reineke J, Tenzer S, Rupnik M, Koschinski A, Hasselmayer O, Schrattenholz A, Schild H, von Eichel-Streiber C. Autocatalytic cleavage of Clostridium difficile toxin B. Nature 2007;446:415–419.

41. Egerer M, Giesemann T, Jank T, Satchell KJ, Aktories K. Auto-catalytic cleavage of Clostridium difficile toxins A and B depends on cysteine protease activity. J Biol Chem 2007;282:25314–25321.

42. Rupnik M, Pabst S, Rupnik M, von Eichel-Streiber C, Urlaub H, Soling HD. Characterization of the cleavage site and function of resulting cleavage fragments after limited proteolysis of Clostridium difficile toxin B (TcdB) by host cells. Microbiology 2005;151:199–208.

43. Pfeifer G, Schirmer J, Leemhuis J, Busch C, Meyer DK, Aktories K, Barth H. Cellular uptake of Clostridium difficile toxin B. Translocation of the N-terminal catalytic domain into the cytosol of eukaryotic cells. J Biol Chem 2003;278:44535–44541.

44. Shen A, Lupardus PJ, Gersch MM, Puri AW, Albrow VE, Garcia KC, Bogyo M. Defining an allosteric circuit in the cysteine protease domain of Clostridium difficile toxins. Nat Struct Mol Biol 2011;18:364–371.

45. Puri AW, Lupardus PJ, Deu E, Albrow VE, Garcia KC, Bogyo M, Shen A. Rational design of inhibitors and activity-based probes targeting Clostridium difficile virulence factor TcdB. Chem Biol 2010;17:1201–1211.

46. Chumbler NM, Farrow MA, Lapierre LA, Franklin JL, Haslam DB, Goldenring JR, Lacy DB. Clostridium difficile toxin B causes epithelial cell necrosis through an autoprocessing-independent mechanism. PLoS Pathog 2012;8:e1003072.

47. Jiang ZD, DuPont HL, Garey K, Price M, Graham G, Okhuysen P, Dao-Tran T, LaRocco M. A common polymorphism in the interleukin 8 gene promoter is associated with Clostridium difficile diarrhea. Am J Gastroenterol 2006;101:1112–1116.

48. El Feghaly RE, Stauber JL, Deych E, Gonzalez C, Tarr PI, Haslam DB. Markers of intestinal inflammation, not bacterial burden, correlate with clinical outcomes in Clostridium difficile infection. Clin Infect Dis 2013; 56:1713–1721.

49. Yacyshyn MB, Reddy TN, Plageman LR, Wu J, Hollar AR, Yacyshyn BR. Clostridium difficile recurrence is characterized by pro-inflammatory peripheral blood mononuclear cell (PBMC) phenotype. J Med Microbiol 2014; 63:1260–1273.

50. Siddiqui F, O'Connor JR, Nagaro K, Cheknis A, Sambol SP, Vedantam G, Gerding DN, Johnson S. Vaccination with parenteral toxoid B protects hamsters against lethal challenge with toxin A-negative, toxin B-positive clostridium difficile but does not prevent colonization. J Infect Dis 2012;205:128–133.

51. Kuehne SA, Cartman ST, Heap JT, Kelly ML, Cockayne A, Minton NP. The role of toxin A and toxin B in Clostridium difficile infection. Nature 2010;467: 711–713.

52. Lawley TD, Clare S, Walker AW, Goulding D, Stabler RA, Croucher N, Mastroeni P, Scott P, Raisen C, Mottram L, Fairweather NF, Wren BW, Parkhill J, Dougan G. Antibiotic treatment of clostridium difficile carrier mice triggers a supershedder state, spore-mediated transmission, and severe disease in immunocompromised hosts. Infect Immun 2009;77:3661–3669.

53. Bender KO, Garland M, Ferreyra JA, Hryckowian AJ, Child MA, Puri AW, Solow-Cordero DE, Higginbottom SK, Segal E, Banaei N, Shen A, Sonnenburg JL, Bogyo M. A small-molecule antivirulence agent for treating Clostridium difficile infection. Sci Transl Med 2015;7:306ra148.

54. Beilhartz GL, Tam J, Zhang Z, Melnyk RA. Comment on "A small-molecule antivirulence agent for treating Clostridium difficile infection". Sci Transl Med 2016;8:370tc2.

**Correspondence**
Address correspondence to: Hanping Feng, PhD, 650 W Baltimore Street, Room 7211, Baltimore, Maryland 21201. e-mail: HFeng@umaryland.edu; fax: (410) 706-6511.

Present affiliation of Z.Y. and H.Y.: FZata, Inc, Halethorpe, Maryland.

**Author contributions**
Yongrong Zhang, Shan Li, Zhiyong Yang, Lianfa Shi, and Hua Yu performed the experiments; Rosangela Salerno-Goncalves provided the 3-dimensional human colonic model; Yongrong Zhang designed the experiments and analyzed data and drafted the manuscript; Hanping Feng conceived the concept of the study and designed experiments; and Hanping Feng and Ashley Saint Fleur revised the manuscript.